

Enhanced tunability in ferroelectric composites through local field enhancement and the effect of disorder

Benjamin Vial and Yang Hao¹

School of Engineering and Computer Science, Queen Mary, University of London, London, E1 4NS, United Kingdom

We investigate **numerically** the homogenized permittivities of **composites** made of low index dielectric inclusions in a ferroelectric matrix under a static electric field. A refined model is used to take into account the coupling between the electrostatic problem and the electric field dependent permittivity of the ferroelectric material, leading to a local field enhancement and permittivity change in the ferroelectric. Periodic and pseudo-random structures in two dimensions are investigated and we **compute** the effective permittivity, losses, electrically induced anisotropy and tunability of those metamaterials. We show that the tunability of such composites might be substantially enhanced in the periodic case, **whereas** introducing disorder in the microstructure weakens the effect of enhanced local permittivity change. Our results may be useful to guide the synthesis of novel composite ceramics with improved characteristics for controllable microwave devices.

1. INTRODUCTION

Ferroelectric materials play a crucial role in reconfigurable microwave devices, with typical applications including antenna beam steering, phase shifters, tunable power splitters, filters, voltage controlled oscillators and matching networks¹. Both bulk ceramics and thin films have been employed to design frequency agile components^{2–4} and metamaterials^{5,6}. The main reason of using ferroelectric materials is their strong dependence of their permittivity ϵ on an applied electric field E , which is measured by their tunability defined as $n = \epsilon(0)/\epsilon(E)$, along with a non hysteresis behaviour when used in their paraelectric state. The key requirements for antenna and microwave applications are large tunability and low losses. These two characteristics are correlated and one has to find a trade-off for optimal device performance, which can be quantified by the so called commutation quality factor $K = (n - 1)^2 / (n \tan \delta(0) \tan \delta(E))$, where $\tan \delta$ is the loss tangent. These materials have usually high permittivity values even at microwave frequencies, often leading to slow response time and impedance mismatch, which can be an issue in some practical applications. Thus it has been considered to mix ferroelectric **ceramics with** low-index and low-loss non-tunable dielectrics in order to reduce both permittivity values and losses, or to use porous ceramics to achieve the same goals without unwanted chemical reactions at the boundaries between dissimilar materials. **In particular, the addition of magnesium oxide in barium strontium titanate (BST) ceramics have been shown to decrease the losses while keeping good tunability^{7,8}. Ceramics such as $\text{Pb}(\text{Zr}, \text{Ti})\text{O}_3$ (PZT) and BaTiO_3 (BT) have been used as fillers in polymer based composites with high dielectric constant⁹. Other mixtures include metal–polymer composites¹⁰ and electroactive polymers such as poly(vinylidene fluoride) (PVDF) with high index dielectric inclusions¹¹.**

The effective parameters of those composites have been investigated^{12–15} and it has been found that the permittivity can be greatly reduced while losses are much less sensitive to the dielectric phase addition, and in some situations lead to a small increase of the tunability of the mixtures. Analytical models based on the Bruggeman effective medium approach

for low concentration of dielectrics were derived for different configurations (columnar, layered and spherical inclusions models) and have been successfully compared with numerical simulations and experiments¹². In the context of porous ferroelectrics, the homogenized properties strongly depends on the size and morphology of the pores^{16,17}. Recently, the concept of tailoring the nonlinear properties of ferroelectric and dielectric structures by local field engineering has been introduced^{18–20}. It was shown through finite element calculation including the nonlinear coupling, that by employing composite materials made of linear dielectric inclusions into a ferroelectric matrix, one can lower the permittivity while maintaining high tunability, due to the local field in the ferroelectric phase which is tuned by the linear dielectric phase. Moreover, the effect of grain sizes in ferroelectric ceramics was studied using a model taking the field enhancement into account at the grain boundaries, and the predicted behaviour successfully compared to experimental data¹⁹. Generally, there is a need for refined theoretical and numerical models to explain and design tunable materials and composites with tailored nonlinear properties. **Note that the general method followed by our coupled model could be applied to other type of tunable systems where local field enhancement and amplification is relevant, including for example ferromagnetic metamaterials²¹, liquid crystals based devices²², or field-enhanced carrier dynamics in doped semiconductors at other frequency ranges, particularly in the THz and near-infrared^{23,24}.**

This study investigates **numerically** the effective permittivity of composites made of dielectric inclusions in a ferroelectric matrix by using a two-scale convergence method^{25,26}. The originality lies in the fact that a fully coupling model is employed to calculate the electrostatic field distribution when a uniform biasing field is applied on the structures, which will result in a local modification of the permittivity in the ferroelectric phase due to the microstructure. As compared to a simple uncoupled model where the ferroelectric phase is only modified through the biasing field, the resulting effective permittivity, dielectric losses, tunability and anisotropy significantly differ. **In contrast with** earlier studies in the **literature^{18,19}**, we account for the non-linear coupling beyond the first iteration and use two-scale convergence homogenization

analysis to obtain the effective parameters at higher frequencies, instead of a capacitance-based model. The model we developed has been implemented with the finite element method (FEM) and we realise a systematic computational study of ferroelectric-dielectric mixtures. First, we consider metamaterials consisting of a square array of parallel dielectric rods with circular cross section in a ferroelectric host, and then investigate the effect of random distribution of those rods within the unit cell.

II. THEORY AND NUMERICAL MODEL

We consider a composite made of a ferroelectric material with anisotropic permittivity $\epsilon^f(\mathbf{E})$ that is dependent on an applied electric field \mathbf{E} , and a non tunable dielectric of permittivity ϵ^d , which are both non-magnetic. The structures under study are invariant along the z direction, which leads to the standard decomposition of the wave equation in the transverse electric case (TE, electric field parallel to the direction of invariance) and the transverse magnetic case (TM, magnetic field parallel to the direction of invariance). A uniform biasing field is applied in order to be able to tune the effective permittivity. Modelling homogenized properties of this type of mixtures can be done by assuming that the electric field distribution is uniform throughout the sample, so that the study of the tunability is essentially achieved by changing the value of the properties in the ferroelectric phase and computing the effective permittivity of the composite. We refer this approach as to the uncoupled model in the following. However, a more accurate description is to take into account the change of the electric field by the microstructure, if any. We therefore need to solve an electrostatic equation to find the field distribution within the material, but its solution depends on the permittivities of both materials, and the permittivity in the ferroelectric phase depends on this induced electric field: this leads to a strongly coupled problem.

A. Permittivity model

We use barium strontium titanate (BST) as our ferroelectric material. $\text{Ba}_x\text{Sr}_{1-x}\text{TiO}_3$ samples were fabricated using the conventional sintering method with a barium ratio of $x = 0.6$ to obtain a dielectrically tunable material as reported in the literature^{11,27}. The tunability was measured using an impedance analyzer up to 100 MHz, and at 3.8 GHz using a loaded microstrip split ring resonator²⁸. The measured tunability of the in-house BST samples of 27% under 1kV/mm DC bias was in agreement with those reported elsewhere^{11,27}. The method presented is however general and only relies on the gradient of the dielectric tunability vs electric field and could be applied to any tunable host material. The normalized permittivity value as a function of biasing field are reported on Fig. (1).

To describe the permittivity, we make use of the Landau potential given by $F(P, E) = F_0 + aP^2/2 + bP^4/4 +$

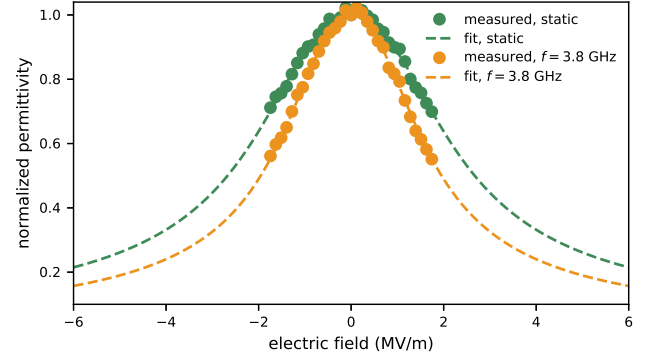


FIG. 1. Variation of the ferroelectric permittivity as a function of the applied electric field (dots: measurements, dashed lines: fit to formula (1)), for the static case (green) and at microwave frequencies (orange, $f = 3.8$ GHz). The fitting parameters are given in Table I.

$cP^6/6 - EP$, where E is the applied electric field and P is the polarization^{29,30}. Variations of the permittivity with the temperature can be taken into account through the coefficients a , b and c , but we assume we are working at a constant room temperature. We further assume that the material is not subject to any stress, so that the variation of permittivity due to mechanical constraints is irrelevant. The equation of state

$$\frac{\partial F(P, E)}{\partial P} = aP_0 + bP_0^3 + cP_0^5 - E = 0$$

gives the dependence of the polarization on the applied electric field, with P_0 being the equilibrium polarization. Along the direction of a uniform applied electric field, the relative permittivity is given by:

$$\epsilon^f(E) = \left[\frac{\partial^2 F(P, E)}{\partial P^2} \right]^{-1} = \frac{\epsilon^f(0)}{1 + \alpha P_0^2 + \beta P_0^4}, \quad (1)$$

where $\epsilon^f(0) = 1/a$, $\alpha = 3b/a$ and $\beta = 5c/a$. The fitting parameters are given in Table I. As the norm of the field increases, the permittivity decreases with a characteristic bell curve typical for a ferroelectric material in its paraelectric state. Furthermore, assuming the crystalline principal axes of the ferroelectric material are oriented in the coordinate directions, and that the diagonal components of the permittivity tensor are only function of the corresponding bias electric field components³¹, we have:

$$\epsilon^f(\mathbf{E}) = \begin{pmatrix} \epsilon_{xx}^f(E_x) & 0 & 0 \\ 0 & \epsilon_{yy}^f(E_y) & 0 \\ 0 & 0 & \epsilon_{zz}^f(E_z) \end{pmatrix} \quad (2)$$

where each of the diagonal components have the functional form given by Eq. (1). Note that we will use the static values of permittivity for the electrostatic modelling, while we are interested in the homogenized values of permittivity at microwaves.

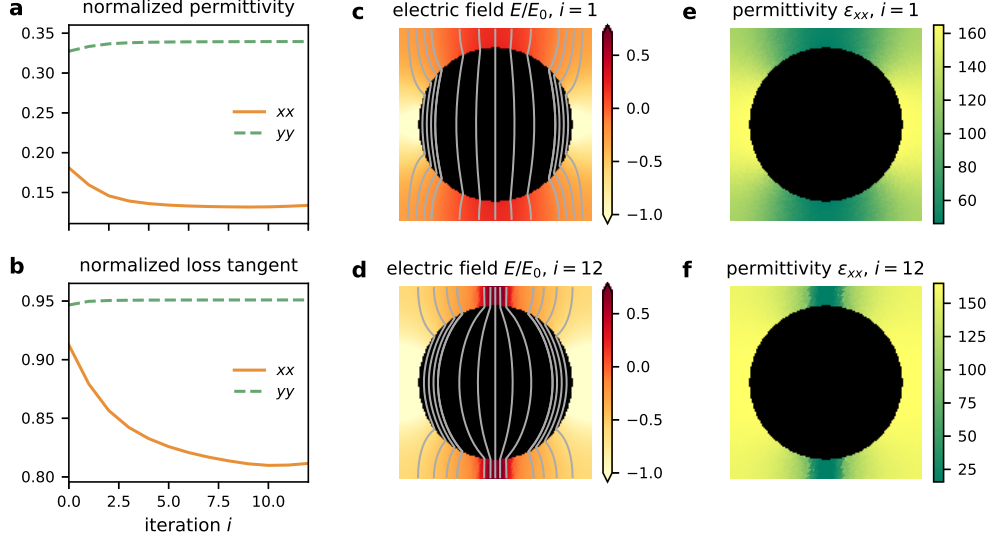


FIG. 2. Convergence of the coupled problem. Real part (a) and loss tangent (b) of the components of the homogenized permittivity tensor as a function of iteration step i . The values are normalized to the corresponding quantities for the bulk ferroelectric material. The distribution of the normalized electric field (colour map: magnitude in logarithmic scale, lines: equipotential contours) and of the xx component of the permittivity tensor are shown for $i = 1$ (c and d) and $i = 12$ (e and f).

TABLE I. Fitting parameters to model (1) for the measured permittivity values as a function of applied electric field shown on Fig. (1).

case	$\epsilon^f(0)$	α ($\mu\text{m}^2/\text{V}^2$)	β ($\mu\text{m}^4/\text{V}^4$)
static	3050	0.120	0.024
$f = 3.8$ GHz	165	0.240	0.079

B. Electrostatic model

The composites under study are made of two materials, thus their permittivity is represented by a piecewise defined tensor $\epsilon(\mathbf{r}, \mathbf{E})$ which is equal to $\epsilon^f(\mathbf{E}(\mathbf{r}))$ in the ferroelectric phase and $\text{diag}(\epsilon^d)$ in the dielectric phase. In the following, we consider two different cases for the biasing field. Because of the form (2) assumed for the ferroelectric permittivity tensor, ϵ_{zz} will not be changing for a field in the plane orthogonal to the z axis. This is the only component being relevant for TE polarization, so we consider in this case a uniform biasing electric field applied along the direction of invariance $\mathbf{E}_0 = E_0 \mathbf{e}_z$. On the other hand, the in-plane components of ϵ^f are tuned by E_x and E_y , therefore, without loss of generality, we consider a uniform applied electric field directed along the x axis $\mathbf{E}_0 = E_0 \mathbf{e}_x$ for the TM polarization case. To calculate the total electric field in the material, one has to solve for the potential V satisfying Gauss' law:

$$\nabla \cdot (\epsilon \nabla V) = 0 \quad (3)$$

Note that for the TE case, the solution is trivial since the structures are invariant along z , so that the electric field is equal to the uniform biasing field, and we will thus not study it in the following. However in the TM case, the situation is much more complex: this is a coupled problem since the

electric field $\mathbf{E} = -\nabla V$ derived from the solution of Eq. (3) depends on the permittivity distribution, which itself depends on the electric field. The coupled system formed of Eqs. (2) and (3) is solved iteratively until there is convergence on the norm of the electric field. Here we would like to emphasise that the permittivity in the ferroelectric material, although uniform initially, is spatially varying due to the non-uniform distribution of the total electric field.

C. Homogenization

When the period of the composite metamaterial is much smaller than the wavelength, one can describe the properties of the composite by a bulk medium with homogenized parameters. The effective permittivity for TM polarization is calculated using a two scale convergence homogenization technique^{25,26}. For this purpose, one has to find the solutions ψ_j of two annex problems \mathcal{P}_j , $j = \{1, 2\}$:

$$\nabla \cdot [\xi \nabla (\psi_j + r_j)] = 0, \quad (4)$$

where $\mathbf{r} = (x, y)^T$ is the position vector in the xy plane and $\xi = \epsilon^T / \det(\epsilon)$. The homogenized tensor $\tilde{\xi}$ is obtained with:

$$\tilde{\xi} = \langle \xi \rangle + \phi, \quad (5)$$

where $\langle \cdot \rangle$ denotes the mean value over the unit cell. The elements of the matrix ϕ represent correction terms and are given by $\phi_{ij} = \langle \xi \nabla \psi_i \rangle_j$. Finally the effective permittivity tensor can be calculated using $\tilde{\epsilon} = \tilde{\xi}^T / \det(\tilde{\xi})$. Note that the TE case, which we shall not study here as no

coupling happens, is trivial since the homogenized permittivity is simply the average of the permittivity in the unit cell: $\tilde{\epsilon} = \langle \epsilon \rangle$.

III. NUMERICAL RESULTS

In the following numerical results, the dielectric phase is supposed to be lossless and non dispersive with $\epsilon^d = 3$ while the ferroelectric material follows the permittivity described in section II A and has a constant loss tangent $\tan \delta^f = 10^{-2}$. Equations (3) and (4) are solved with a Finite Element Method using the open source packages Gmsh³² and GetDP³³. In both cases we use a square unit cell Ω of length d with periodic boundary conditions along x and y . Second order Lagrange elements are used and the solution is computed with a direct solver (MUMPS³⁴).

A. Two dimensional periodic metamaterial

Lets us now consider a periodic square array of infinitely long dielectric rods of circular cross section of radius r embedded in a ferroelectric matrix.

We first study the convergence of the coupled problem on the particular case with dielectric filling fraction $f = \pi r^2/d^2 = 0.5$ and $E_0 = 2\text{MV/m}$. Figures 2(a) and 2(b) show the convergence of the real part and loss tangent of the components of the homogenized permittivity tensor, respectively. The yy components converge quickly and are almost unaffected by the coupling process whereas the xx components change substantially from the initial conditions. This is due to the effect of the redistribution of the electrostatic field within the unit cell (see Figs. (2.c) and (2.d)), where the x component of the electric field is still much stronger than the y component, even if spatially varying in the ferroelectric medium. At equilibrium, the electric field is concentrated close to the y axis in between two neighbouring rods. This in turn affects the permittivity distribution (see Figs. (2.e) and (2.f)), and the homogenized properties of the composite.

We computed the effective parameters of these metamaterial structures for different radii of the rods and studied their behaviour when subjected to an external electrostatic field (see Fig. (3)). The results of our coupled model differ significantly from the uncoupled one. Increasing the dielectric fraction lowers the effective permittivity while the losses are slightly reduced but much less sensitive. Due to the inhomogeneous redistribution of the permittivity over the ferroelectric domain, the overall tunability changes. In the case studied here, taking into account the coupling leads to an effective tunability increase with higher dielectric concentration, and that is larger than the tunability of bulk ferroelectric. This can be seen in Fig. (3).c where we plot the tunability of the composites along the x axis, $\tilde{n}(E) = \tilde{\epsilon}_{xx}(E)/\tilde{\epsilon}_{xx}(0)$, normalized to the tunability of the bulk ferroelectric $n(E) = \epsilon_{xx}^f(E)/\epsilon_{xx}^f(0)$. Two concurrent effects are at stake here: on the one hand the dilution of ferroelectric makes the composite less tunable, but on the other hand, the rearrangement of the electrostatic field sur-

rounding the inclusion and its concentration in some region will cause a higher permittivity change locally. The relative strength of those phenomena is governed by the shape of the inclusion and its permittivity and so it is envisioned that the performance of the composites might be enhanced by engineering their microstructure. The geometry of the unit cell is symmetric so the homogenized material is isotropic when no field is applied. But when the sample is biased, the permittivity distribution becomes asymmetric due to the inhomogeneity of the electric field, thus making the effective material properties anisotropic. This geometric effect is added to the anisotropy arising from the material properties of the ferroelectric phase itself, and depending on the topology and permittivity of the rods, one effect would be predominant. In the case studied here, the equilibrium permittivity distribution varies strongly along the bias direction and much less orthogonally to it, which adds anisotropy by diminishing the effective permittivity in the x direction. This is local field induced effect is what makes the anisotropy stronger in our coupled model compared to the uncoupled one (cf. Fig. (3.d) where we plot the anisotropy factor $\alpha = \epsilon_{xx}/\epsilon_{yy}$). Those subtle phenomena can only be rigorously taken into account by employing a coupling formalism and are responsible for the difference observed when compared to a simple uncoupled model.

B. Pseudo-random case

We finally study the effect of random distribution of the inclusions within the unit cell on the effective parameters of the composites. This is an important point as fabrication of randomly dispersed inclusions is much more easy from a technological perspective. For each filling fraction of the dielectric, we generated 21 numerical samples with inclusions of circular cross section of average radius $r = d/20$ that can vary by $\pm 30\%$. Their centre is chosen randomly and the rods are allowed to overlap. An example of distribution for $f = 0.5$ is given on Fig. (6). The effective material properties are plotted on Fig. (4). Similarly to the periodic case, the permittivity decreases with increasing dilution of ferroelectric, but for identical filling fraction, the permittivity is lower as compared to the periodic array, and the smaller the dielectric concentration the larger is the difference. Losses decrease as well and the reduction is substantially larger than the periodic case, with higher variation from sample to sample as f increases. The effective tunability is on average smaller than that in the periodic case, and for low biasing fields and for some particular samples can be greater than the bulk tunability. However, at higher applied electric fields, normalized tunability becomes smaller than unity and is reduced as one adds more dielectric. For comparison, the homogenized parameters are plotted on Fig. (7) in the case where the coupling is neglected. One can see that the coupled and uncoupled models give similar results for the tunability whereas the losses are still smaller for the coupled case at higher fields.

The redistribution of electric field, permittivity and convergence of the effective parameters are displayed in Fig. (5).

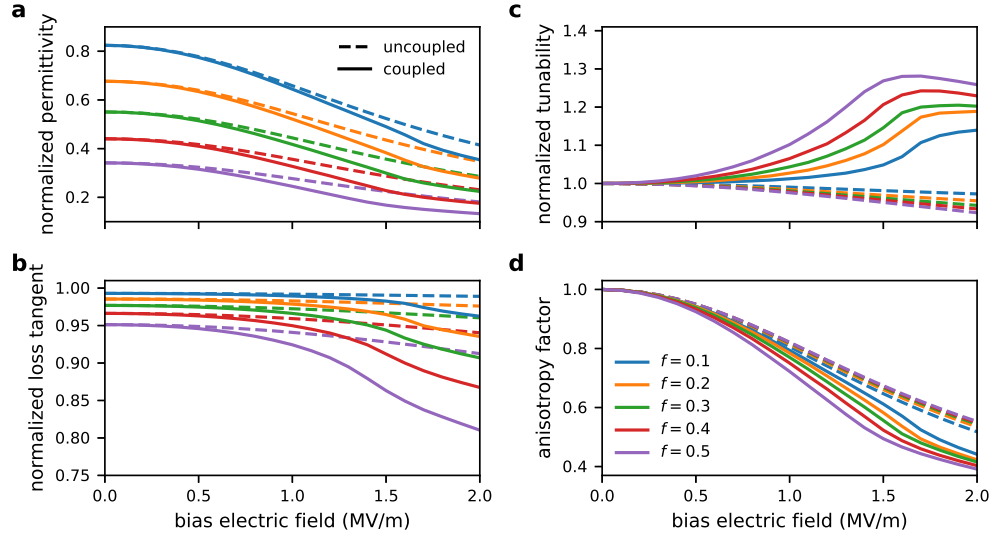


FIG. 3. Effective parameters of the 2D metamaterials as a function of the applied electric field for various filling fraction of dielectric. (a): normalized permittivity, (b): normalized loss tangent, (c): normalized tunability and (d): anisotropy factor. The solid lines correspond to the coupled model and the dashed lines to the uncoupled model. The values are normalized to the corresponding quantities for the bulk ferroelectric material.

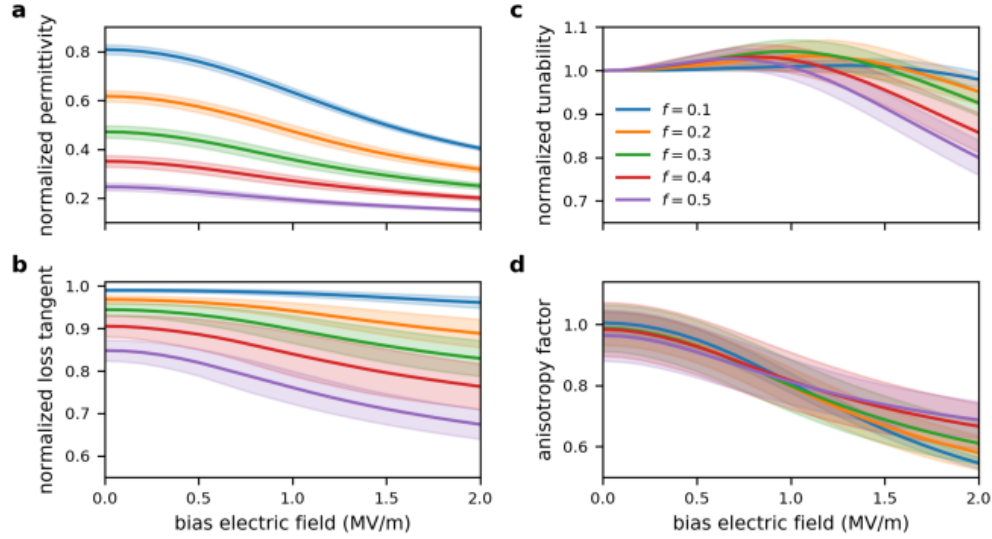


FIG. 4. Effective parameters of the pseudo-random composites as a function of the applied electric field for various filling fraction of dielectric, when the coupling is taken into account. (a): normalized permittivity, (b): normalized loss tangent, (c): normalized tunability and (d): anisotropy factor. The solid lines represent the average values over the 21 samples and the lighter error bands show a confidence interval corresponding to the standard deviation. The values are normalized to the corresponding quantities for the bulk ferroelectric material.

297 The effect of disorder plays an important role here: the elec- 305
 298 trostatic field gets concentrated in between neighbouring in- 306
 299 clusions and the smaller the gap the higher the field, hence 307
 300 a greater local permittivity change. In addition, even if the 308
 301 distribution is random, one expects that the anisotropy due to 309
 302 geometry would cancel for a sufficiently large number of rods 310
 303 (which is the case as the mean anisotropy factor is close to 1 311
 304 when no bias field is applied). However, the anisotropy due 312
 to ferroelectric properties is important in this case as well, as
 both the x and y components of the electrostatic field are play-
 ing a role. Because of the relative positions of the rods, both
 ϵ_{xx} and ϵ_{yy} are affected by the coupling, so that the anisotropy
 factor for higher fields is reduced as compared to the periodic
 case. However even if there is a substantial variability from
 sample to sample, on average, the anisotropy factor decreases
 with increasing dielectric concentration.

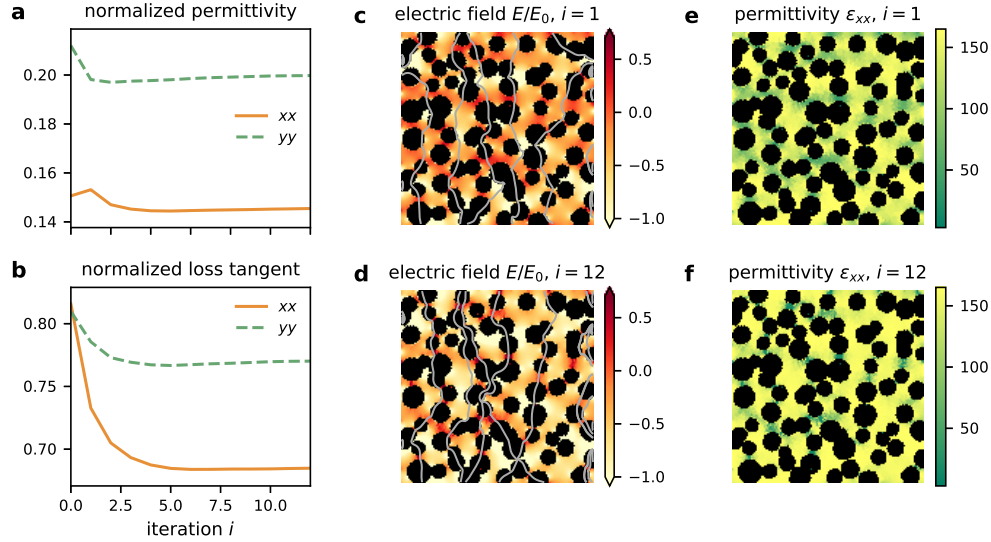


FIG. 5. Convergence of the coupled problem in the random case for one sample. Real part (a) and loss tangent (b) of the components of the homogenized permittivity tensor as a function of iteration step i . The values are normalized to the corresponding quantities for the bulk ferroelectric material. The distribution of the normalized electric field (colour map: magnitude in logarithmic scale, lines: equipotential contours) and of the xx component of the permittivity tensor are shown for $i = 1$ (c and d) and $i = 12$ (e and f).

IV. CONCLUSION

We have studied the homogenized properties of dielectric/ferroelectric mixtures using a rigorous model that take into account the coupling between the electrostatic field distribution and the field dependant ferroelectric permittivity tensor. After convergence of the coupled problem, the effective permittivity tensor is calculated using two scale convergence homogenization theory. The results obtained by this model differ significantly from a simple assumption that the permittivity of the ferroelectric respond just to the uniform biasing field. We have considered both periodic and random arrays of dielectric rods in a ferroelectric matrix in 2D, and studied their effective properties for TM polarization as a function of dielectric concentration and bias field. Importantly, adding more low index and low loss dielectric allows to decrease the overall permittivity significantly and slightly lower the losses. For the periodic case, the tunability is higher than the bulk due to local field enhancement, whereas this effect is strongly suppressed when disorder is introduced. The asymmetric redistribution of the permittivity induce an effective anisotropy that is added to the one arising purely from the ferroelectric material. The properties of the composites are affected by multiple factors: geometry and the spatially dependent electric field that will induce locally a tunable, anisotropic response in the ferroelectric phase depending on its amplitude and direction. This suggest that the performances of the composites may be enhanced by distributing the two phases in an optimal way to get high tunability and low losses. Further work in that direction is needed as well as extending this study to 3D media. Finally, because the permittivity of the dielectric is much smaller

than the ferroelectric one, it would be of great interest to use high contrast homogenization theory^{35,36} to study this kind of mixtures. This would reveal the frequency dependant artificial magnetism due to "micro-resonances" in the high index phase and potentially lead to composites with tunable effective permeability.

ACKNOWLEDGMENTS

This work was funded by the Engineering and Physical Sciences Research Council (EPSRC), UK, under a grant (EP/P005578/1) "Adaptive Tools for Electromagnetics and Materials Modelling to Bridge the Gap between Design and Manufacturing (AOTOMAT)".

The authors would like to thanks Henry Giddens for performing the measurements of ferroelectric permittivity used in this paper.

The codes necessary to reproduce the results in this article are freely available online at this address: <https://www.github.com/benvial/ferromtm>.

¹A. K. Tagantsev, V. O. Sherman, K. F. Astafiev, J. Venkatesh, and N. Setter, "Ferroelectric Materials for Microwave Tunable Applications," J Electroceram **11**, 5–66 (2018).

²O. Vendik, E. Hollmann, A. Kozyrev, and A. Prudan, "Ferroelectric tuning of planar and bulk microwave devices," J. Supercond. **12**, 325–338 (1999).

³M. Lancaster, J. Powell, and A. Porch, "Thin-film ferroelectric microwave devices," Supercond. Sci. Technol. **11**, 1323 (1998).

⁴X. Xi, H.-C. Li, W. Si, A. Sirenko, I. Akimov, J. Fox, A. Clark, and J. Hao, "Oxide thin films for tunable microwave devices," J. Electroceramics **4**, 393–405 (2000).

- ⁵T. H. Hand and S. A. Cummer, "Frequency tunable electromagnetic material using ferroelectric loaded split rings," *J. Appl. Phys.* **103**, 066105 (2008).
- ⁶H. Zhao, L. Kang, J. Zhou, Q. Zhao, L. Li, L. Peng, and Y. Bai, "Experimental demonstration of tunable negative phase velocity and negative refraction in a ferromagnetic/ferroelectric composite metamaterial," *Appl. Phys. Lett.* **93**, 201106 (2008).
- ⁷P. Irvin, J. Levy, R. Guo, and A. Bhalla, "Three-dimensional polarization imaging of (Ba,Sr)TiO₃:MgO composites," *Appl. Phys. Lett.* **86**, 042903 (2005).
- ⁸U.-C. Chung, C. Elissalde, M. Maglione, C. Estournès, M. Paté, and J. P. Ganne, "Low-losses, highly tunable Ba_{0.6}Sr_{0.4}TiO₃ / MgO composite," *Appl. Phys. Lett.* **92**, 042902 (2008).
- ⁹B. Wang, L. Luo, F. Ni, P. Du, W. Li, and H. Chen, "Piezoelectric and ferroelectric properties of (Bi_{1-x}Na_{0.8}0.2)0.5 TiO₃ lead-free ceramics," *Journal of Alloys and Compounds* **526**, 79–84 (2012).
- ¹⁰X. Li, Y.-F. Lim, K. Yao, F. E. H. Tay, and K. H. Seah, "Ferroelectric Poly(vinylidene fluoride) Homopolymer Nanotubes Derived from Solution in Anodic Alumina Membrane Template," *Chem. Mater.* **25**, 524–529 (2013).
- ¹¹G. Hu, F. Gao, J. Kong, S. Yang, Q. Zhang, Z. Liu, Y. Zhang, and H. Sun, "Preparation and dielectric properties of poly(vinylidene fluoride)/Ba_{0.6}Sr_{0.4}TiO₃ composites," *Journal of Alloys and Compounds* **619**, 686–692 (2015).
- ¹²V. O. Sherman, A. K. Tagantsev, N. Setter, D. Iddles, and T. Price, "Ferroelectric-dielectric tunable composites," *J. Appl. Phys.* **99**, 074104 (2006).
- ¹³L. Jylha and A. H. Sihvola, "Tunability of granular ferroelectric dielectric composites," *Prog. Electromagn. Res.* **78**, 189–207 (2008).
- ¹⁴V. O. Sherman, A. K. Tagantsev, and N. Setter, "Tunability and loss of the ferroelectric-dielectric composites," in *14th IEEE International Symposium on Applications of Ferroelectrics, 2004. ISAF-04. 2004* (2004) pp. 33–38.
- ¹⁵K. F. Astafiev, V. O. Sherman, A. K. Tagantsev, and N. Setter, "Can the addition of a dielectric improve the figure of merit of a tunable material?" *J. Eur. Ceram. Soc.* **23**, 2381–2386 (2003).
- ¹⁶K. Okazaki and K. Nagata, "Effects of Grain Size and Porosity on Electrical and Optical Properties of PLZT Ceramics," *J. Am. Ceram. Soc.* **56**, 82–86 (1973).
- ¹⁷R. Stanculescu, C. E. Ciomaga, L. Padurariu, P. Galizia, N. Horchidan, C. Capiati, C. Galassi, and L. Mitoseriu, "Study of the role of porosity on the functional properties of (Ba,Sr)TiO₃ ceramics," *J. Alloys Compd.* **643**, 79–87 (2015).
- ¹⁸L. Padurariu, L. Curecheriu, C. Galassi, and L. Mitoseriu, "Tailoring nonlinear dielectric properties by local field engineering in anisotropic porous ferroelectric structures," *Appl Phys Lett* **100**, 252905 (2012).
- ¹⁹L. Padurariu, L. Curecheriu, V. Buscaglia, and L. Mitoseriu, "Field-dependent permittivity in nanostructured BaTiO₃ ceramics: Modeling and experimental verification," *Phys Rev B* **85**, 224111 (2012).
- ²⁰A. Cazacu, L. Curecheriu, A. Neagu, L. Padurariu, A. Cernescu, I. Lisiecki, and L. Mitoseriu, "Tunable gold-chitosan nanocomposites by local field engineering," *Appl Phys Lett* **102**, 222903 (2013).
- ²¹L. Carignan, A. Yelon, D. Menard, and C. Caloz, "Ferromagnetic Nanowire Metamaterials: Theory and Applications," *IEEE Trans. Microw. Theory Tech.* **59**, 2568–2586 (2011).
- ²²D. H. Werner, D.-H. Kwon, I.-C. Khoo, A. V. Kildishev, and V. M. Shalaev, "Liquid crystal clad near-infrared metamaterials with tunable negative-zero-positive refractive indices," *Opt. Express, OE* **15**, 3342–3347 (2007).
- ²³G. R. Keiser and P. Klarskov, "Terahertz Field Confinement in Nonlinear Metamaterials and Near-Field Imaging," *Photonics* **6**, 22 (2019).
- ²⁴K. Fan, H. Y. Hwang, M. Liu, A. C. Strikwerda, A. Sternbach, J. Zhang, X. Zhao, X. Zhang, K. A. Nelson, and R. D. Averitt, "Nonlinear Terahertz Metamaterials via Field-Enhanced Carrier Dynamics in GaAs," *Phys. Rev. Lett.* **110**, 217404 (2013).
- ²⁵G. Allaire, "Homogenization and Two-Scale Convergence," *SIAM J. Math. Anal.* **23**, 1482–1518 (1992).
- ²⁶S. Guenneau and F. Zolla, "Homogenization of Three-Dimensional Finite Photonic Crystals," *J. Electromagn. Waves Appl.* **14**, 529–530 (2000).
- ²⁷S. Agrawal, R. Guo, D. Agrawal, and A. S. Bhalla, "Tunable BST:MgO Dielectric Composite by Microwave Sintering," *Ferroelectrics* **306**, 155–163 (2004).
- ²⁸M. A. H. Ansari, A. K. Jha, and M. J. Akhtar, "Design and Application of the CSRR-Based Planar Sensor for Noninvasive Measurement of Complex Permittivity," *IEEE Sens. J.* **15**, 7181–7189 (2015).
- ²⁹L. D. Landau, J. Bell, M. Kearsley, L. Pitaevskii, E. Lifshitz, and J. Sykes, *Electrodynamics of continuous media*, Vol. 8 (elsevier, 2013).
- ³⁰K. Zhou, S. A. Boggs, R. Ramprasad, M. Aindow, C. Erkey, and S. P. Alpay, "Dielectric response and tunability of a dielectric-paraelectric composite," *Appl. Phys. Lett.* **93**, 102908 (2008).
- ³¹C. M. Krowne, M. Daniel, S. W. Kirchoefer, and J. A. Pond, "Anisotropic permittivity and attenuation extraction from propagation constant measurements using an anisotropic full-wave Green's function solver for coplanar ferroelectric thin-film devices," *IEEE Trans. Microw. Theory Tech.* **50**, 537–548 (2002).
- ³²C. Geuzaine and J.-F. Remacle, "Gmsh: A 3-D finite element mesh generator with built-in pre- and post-processing facilities," *Int. J. Numer. Methods Eng.* **79**, 1309–1331 (2009).
- ³³P. Dular, C. Geuzaine, F. Henrotte, and W. Legros, "A general environment for the treatment of discrete problems and its application to the finite element method," *IEEE Trans. Magn.* **34**, 3395–3398 (1998).
- ³⁴P. R. Amestoy, I. S. Duff, J. Koster, and J.-Y. L'Excellent, "A Fully Asynchronous Multifrontal Solver Using Distributed Dynamic Scheduling," *SIAM J. Matrix Anal. Appl.* **23**, 15–41 (2001).
- ³⁵G. Bouchitté and D. Felbacq, "Homogenization near resonances and artificial magnetism from dielectrics," *Comptes Rendus Mathématique* **339**, 377–382 (2004).
- ³⁶K. Cherednichenko and S. Cooper, "Homogenization of the system of high-contrast Maxwell equations," *Mathematika* **61**, 475–500 (2015).

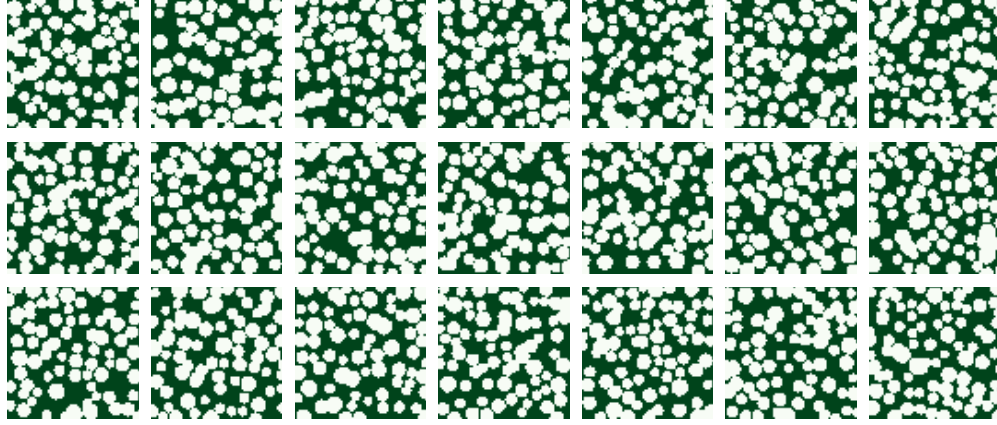
Random material samples, $f = 0.5$ 

FIG. 6. Permittivity distribution of the numerical samples used for $f = 0.5$. Dark colour indicates the ferroelectric material while light colour represents the dielectric inclusions.

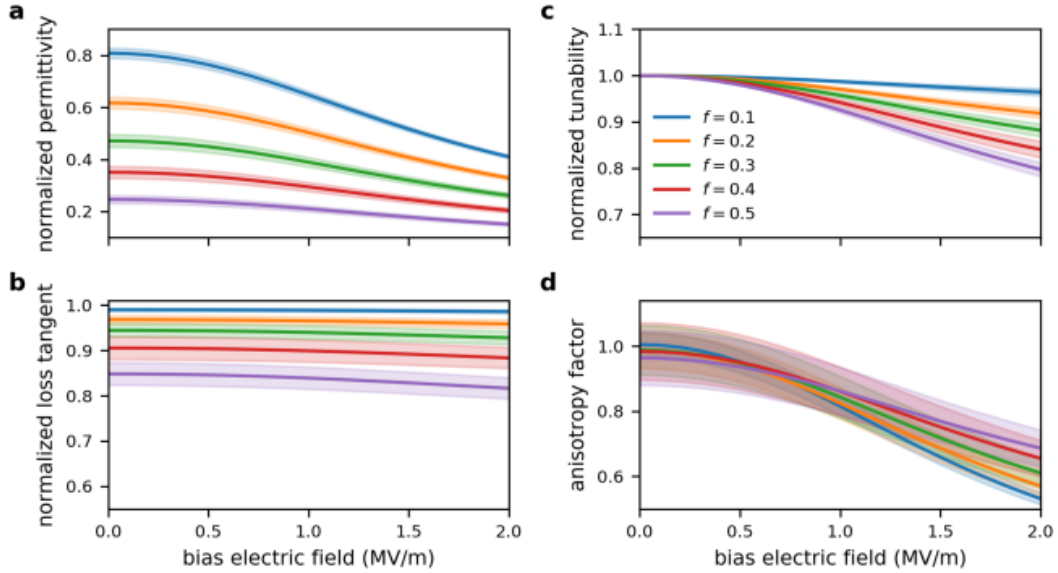


FIG. 7. Effective parameters of the random 2D mixtures as a function of the applied electric field for various filling fraction of dielectric, when the coupling is neglected. (a): normalized permittivity, (b): normalized loss tangent, (c): normalized tunability and (d): anisotropy factor. The solid lines represent the average values over the 21 samples and the lighter error bands show a confidence interval corresponding to the standard deviation. The values are normalized to the corresponding quantities for the bulk ferroelectric material.